Enhanced adsorption of nitrate from water by modified wheat straw: equilibrium, kinetic and thermodynamic studies

Behrouz Mehdinejadiani, Seyed Mojtaba Amininasab and Leila Manhooei

ABSTRACT

This study represents the first attempt to chemically modify wheat straw (WS) using 3-chloropropyltrimethoxysilane (CPTMS) and (1,4-diazabicyclo[2.2.2]octane) (DABCO). Field emission scanning electron micrographs (FESEM), energy dispersive spectroscopy (EDS), thermogravimetric analysis (TGA) and Fourier transform infrared (FTIR) spectra confirmed the successful morphological and structural modification of WS and the thermal stability of the modified WS (MWS). The MWS was used to remove nitrate from water. The optimum conditions of nitrate adsorption onto MWS were examined by conducting batch experiments. The results indicated that 85% of nitrate was removed under the conditions of initial nitrate concentration $= 20$ mg L^{-1}, initial solution pH $= 7$, contact time $= 10$ min, MWS dosage $= 2$ g L^{-1} and temperature $\approx 25\,°$C. The kinetic adsorption data were best fitted to the general order model and the adsorption process occurred in three distinct stages. The equilibrium adsorption data were well described by the Langmuir isotherm. Additionally, separation factor values were smaller than 1, implying that the adsorption process was favorable. The presence of competing anions impeded the nitrate adsorption in the order of sulfate > chloride > bicarbonate> phosphate. Thermodynamic parameters suggested that the adsorption process was exothermic, feasible and spontaneous in nature. Overall, the MWS could achieve efficient removal of nitrate under the simplest operating conditions.

Key words | 3-chloropropyltrimethoxysilane (CPTMS), agricultural by-product, general order kinetic model, Langmuir isotherm model, nonlinear fitting

Behrouz Mehdinejadiani (corresponding author)
Leila Manhooei
Department of Water Science and Engineering,
   Faculty of Agriculture,
University of Kurdistan,
Sanandaj,
Iran
E-mail: b.mehdinejad@uok.ac.ir

Seyed Mojtaba Amininasab
Polymer Chemistry Research Laboratory,
   Department of Chemistry, Faculty of Science,
University of Kurdistan,
Sanandaj,
Iran

INTRODUCTION

Nitrate pollution of water resources has become a major concern in agricultural regions (Sepehri et al. 2014). The World Health Organization (WHO) standard has set the allowable maximum concentration of nitrate in drinking water at 50 mg L^{-1} (WHO 2011). The high concentration of nitrate in water causes methemoglobinemia in infants, some cancers in adults and teratogenic effects (Rezaei Kalantary et al. 2016). Considering the adverse effects of excessive nitrate in water, its removal from water resources is of great importance. Anion exchange is an effective process for treating nitrate-contaminated water, which can be utilized in small to medium sized treatment plants (Bergquist et al. 2016). In recent years, many attempts have been made to produce local, inexpensive and effective anion exchangers from agricultural by-products such as rice husk (Katal et al. 2012), wheat straw (Xue et al. 2016),

pine sawdust (Keränen 2017), sugarcane bagasse biochar (Divband Hafshejani et al. 2016) and granular activated carbon (Mazarji et al. 2017).

Wheat has the third highest global production after maize and rice, and Iran has the eleventh rank of wheat production in the world (FAOSTAT 2013). In Iran, about 50% of total production is lost as waste, especially in the form of straw (Najafi et al. 2012). The wheat straw (WS) is a complex mixture of cellulose, hemicellulose, lignin, pectin, protein and fatty acid. These components contain multiple functional groups of hydroxyls, carboxyl, ether, amino and phosphate (Wang et al. 2016). Furthermore, the vascular bundle structure of WS gives additional surface for chemical modification (Ebrahimian Pirbazari et al. 2014). Due to having these properties, the raw WS and the chemically modified WS (MWS) have been used for removal

of different contaminants from water. Wang *et al.* (2007) prepared an anionic sorbent by cross-linking WS with epichlorohydrin and dimethylamine in the presence of N,N-dimethylformamide and using a pyridine catalyst. According to this study, the maximum adsorption capacity of the MWS for nitrate was 128.97 mg g^{-1}. Xu *et al.* (2011) modified the fermented WS with epichlorohydrin, ethylenediamine and triethylamine in the presence of N,N dimethylformamide, and applied the modified FWS (MFWS) to remove phosphate and chromium (VI) from water. They reported the adsorption capacities of 1.71 mmol g^{-1} for chromium (VI) and 5.68 mmol g^{-1} for phosphate on the MFWS. Li *et al.* (2016) applied WS biochar activated with hydrochloric acid (HCl) and coated with different FeCl$_3$.6H$_2$O amounts to remove nitrate and phosphate from water. According to the obtained results, the MWS biochar removed nitrate and phosphate successfully from water when the optimal ratio of iron to biochar for iron-coated biochar (0.7) was used. Mg-Fe layered double hydroxide (MgFe-LDH) particles were incorporated into WS biochar to synthesize WS biochar/MgFe-LDH adsorbent (Xue *et al.* 2016). This adsorbent removed nitrate efficiently from aqueous solutions and the Langmuir maximum adsorption capacity was found to be 24.8 mg g^{-1}.

In addition to the above-mentioned works, other experimental studies related to the application of chemical materials to modify the WS have been performed (e.g. Ebrahimian Pirbazari *et al.* 2014; Wang *et al.* 2016) that are not mentioned here for the sake of brevity. However, to the authors' knowledge, no relevant reports have been published up to now about the modification of WS with silane groups and the application of the resultant MWS to remove nitrate from water. 3-chloropropyltrimethoxysilane (CPTMS) is a silane coupling agent that is less hazardous in comparison with other chemical materials applied to modify WS, such as epichlorohydrin (Wang *et al.* 2007; Xu *et al.* 2011), FeCl$_3$.6H$_2$O (Li *et al.* 2016; Xue *et al.* 2016), FeSO$_4$.7H$_2$O (Ebrahimian Pirbazari *et al.* 2014) and chloroacetic acid (Wang *et al.* 2016). In this sense, the objectives of this study were to: (1) modify WS using CPTMS and (1,4-diazabicyclo[2.2.2]octane) (DABCO); (2) characterize the physicochemical properties of WS and MWS by field emission scanning electron micrographs (FESEM), energy dispersive spectroscopy (EDS), Fourier transform infrared (FTIR) and thermogravimetric analysis (TGA); (3) investigate the adsorption behavior of nitrate onto MWS under different operational conditions, including initial solution pH, contact time, adsorbent dosage, initial nitrate concentration, presence of competing anions and temperature,

and (4) determine the best kinetic and equilibrium isotherm models describing experimental data.

MATERIALS AND METHODS

Materials and reagents

The WS used in this study was obtained from a local field in Dehgolan, Kudristan province, Iran. The WS was rinsed with distilled water and dried at 60 °C for 12 h. The oven-dried WS was chopped, milled and sieved into particles ranging from 70–200 μm.

The chemical materials utilized in this study included CPTMS, DABCO, toluene, potassium nitrate (KNO$_3$), hydrochloric acid (HCl), sodium hydroxide (NaOH), magnesium sulfate (MgSO$_4$), sodium hydrogen carbonate (NaHCO$_3$), potassium dihydrogen phosphate (KH$_2$PO$_4$) and ammonium chloride (NH$_4$Cl). All of the chemical materials were purchased from Merck (Germany) and used without additional purification. Also, deionized water was used to prepare all solutions.

Modification process of WS

To chemically modify WS, a silanated intermediate was prepared first. The silanated intermediate was synthesized by nucleophilic substitution reaction between amine and alkyl halide groups, wherein an aliquot of 0.56 g of DABCO was reacted with 1.82 ml of CPTMS in 10 ml of toluene solvent at 80 °C under N$_2$ flow. Then, the mixture was stirred for 12 h and finally the intermediate was gathered. After synthesizing the silanated intermediate, a condensation reaction between hydroxyl groups of WS and methoxysilane occurred to produce MWS. In this reaction, 2 g of WS reacted with 2 g of intermediate and 10 ml of acetic acid/ethanol solution (1:9 V/V) in a 100 ml two-neck round-bottom flask for 12 h at 80 °C. For elimination of residual chemicals, the product was washed with 100 ml of ethanol/distilled water (50:50 V/V). The washed product was dried at 60 °C for 12 h, ground and sieved to obtain powder smaller than 200 μm.

Equipment and characterizations

Morphology and element distributions of WS before and after modification were characterized by FESEM using a Mighty-8 instrument (TSCAN Company, Prague) equipped with an EDS detector. Thermogravimetric analyses (TGA)

for WS and MWS were carried out with a DuPont Instruments (TGA 951) analyzer at a heating rate of 10 °C/min from room temperature ($\sim$25 °C) to 700 °C under nitrogen flow. Infrared spectra of WS and MWS were detected by a FTIR spectrometer (FTIR, Bruker Tensor 27 spectrometer, Germany) using the KBr method. A pH meter (Inolab pH 7110, WTW, Weilheim, Germany) was used to measure the pH values of the solutions and a magnetic mixer (IKA RH basic2, Germany) was applied to stir the samples. The concentration of nitrate in the solutions was measured using a UV-vis spectrophotometer (SPECORD 210 Plus, Analytic Jena, Germany).

Investigation of nitrate adsorption process onto MWS

Batch adsorption experiments

The batch adsorption experiments were carried out to determine the effects of various operational factors such as initial solution pH, contact time, adsorbent dosage, initial nitrate concentration, competing anions and temperature on the nitrate adsorption by MWS. At each batch experiment, one of the factors varied and the others were fixed. Preliminary experiments showed that the nitrate removal from water by WS was trivial. Hence, the batch adsorption experiments were only conducted using the MWS.

Six series of batch experiments were carried out. Table 1 shows the operational conditions in each batch experiment. Each batch adsorption experiment was performed in a volumetric flask that contained 50 mL of nitrate solution at a desirable concentration. The nitrate solutions with the required concentrations were prepared from serial dilution of 1,000 mg L^{-1} nitrate stock solution. After adjusting the variable factor and fixing the others, the mixture was continuously stirred using the magnetic mixer at 120 rpm for a desirable contact time. Then, the sample was passed through Whatman 42 filter paper and the residual nitrate concentration in the filtrate solution was determined using the spectrophotometer. Reproducibility of results was checked by performing the experiments in triplicate, and average values were reported.

In the batch experiments, the amount of nitrate adsorbed per unit mass of MWS (adsorption capacity of nitrate onto the MWS) at time t, q_t (mg g^{-1}), and at equilibrium, q_e (mg g^{-1}), as well as the removal percentage of nitrate at equilibrium, R (%), were calculated using the following equations:

$$q_t = \frac{C_i - C_t}{m} \times V \tag{1}$$

$$q_e = \frac{C_i - C_e}{m} \times V \tag{2}$$

$$R(\%) = \frac{C_i - C_e}{C_i} \times 100 \tag{3}$$

where C_i is the initial nitrate concentration (mg L^{-1}); C_t and C_e are the residual nitrate concentrations at time t and at equilibrium (mg L^{-1}); V is the solution volume (L) and m is the adsorbent mass (g).

Table 1 | Conditions of batch experiments

| Run | Experiment | Operational conditions | | | | | |
		pH	Contact time (min)	MWS dosage (g L^{-1})	Initial nitrate concentration (mg L^{-1})	Presence of competing anion (mg L^{-1})	Temperature (°C)
1	Influence of initial solution pH	3–11	120	2	20	No	$\sim$25
2	Influence of contact time	7	2–50	2	20	No	$\sim$25
3	Influence of MWS dosage	7	10	0.25–3	20	No	$\sim$25
4	Influence of initial nitrate concentration	7	10	2	20–150	No	$\sim$25
5	Influence of sulfate (as a competing anion)	7	10	2	20	20, 50, 100	$\sim$25
	Influence of chloride (as a competing anion)	7	10	2	20	20, 50, 100	$\sim$25
	Influence of bicarbonate (as a competing anion)	7	10	2	20	20, 50, 100	$\sim$25
	Influence of phosphate (as a competing anion)	7	10	2	20	20, 50, 100	$\sim$25
6	Influence of temperature	7	10	2	20	No	$\sim$25, 35, 50

Adsorption kinetic studies

See Supplementary material (available with the online version of this paper).

Adsorption equilibrium studies

See Supplementary material.

Statistical evaluation of the kinetic and isotherm parameters

The parameters of the kinetic and isotherm models were estimated using a nonlinear optimization method, except for the intra-particle diffusion (IPD) model. To this end, the kinetic and isotherm models were fitted to the experimental data using the '*Solver add-in*', Microsoft Office Excel (2016 version) (Tran *et al.* 2017). After estimating the parameters, the best-fit kinetic and isotherm models were identified using the following statistical criteria:

Chi-square (χ^2) test (Wang 2012):

$$Chi^2/df(\%) = \frac{\chi^2}{n-p}(\%) = \frac{100}{n-p} \times \sum_{i=1}^{n} \frac{(q_{i,\exp} - q_{i,cal})^2}{q_{i,cal}} \quad (4)$$

Marquardt's percent standard deviation error function (F_{error}) (Wang 2012):

$$F_{error}(\%) = 100 \times \sqrt{\frac{1}{n-p} \cdot \sum_{i=1}^{n} \left(\frac{q_{i,\exp} - q_{i,cal}}{q_{i,\exp}}\right)^2} \quad (5)$$

Adjusted determination coefficient (R^2_{adj}) (Lima *et al.* 2015):

$$R^2_{adj} = 1 - \frac{\sum_{i=1}^{n}(q_{i,\exp} - q_{i,cal})^2}{\sum_{i=1}^{n}(q_{i,\exp} - \bar{q}_{i,\exp})^2} \cdot \left(\frac{n-1}{n-p-1}\right) \quad (6)$$

where df is the degree of freedom; $q_{i,\exp}$ is each value of q experimentally measured; $q_{i,cal}$ is each value of q predicted by the fitted model; $\bar{q}_{\exp}$ is the average of measured values of q; n is the number of measurement points and p is the number of the fitted model parameters. Note that the best fit model is one that has the lowest values of Chi^2/df and F_{error}, as well as having a value of R^2_{adj} closer to unity (Wang 2012; Lima *et al.* 2015).

It is necessary to mention here that the parameters of the IPD model were obtained by means of a plot of q_t versus the square root of contact time (Mazarji *et al.* 2017).

Estimation of thermodynamic parameters

See Supplementary material.

Desorption and reusability studies of MWS

The regeneration of an adsorbent is important from the commercial application perspective. Therefore, the desorption and reusability of MWS for nitrate adsorption were examined. The desorption study was carried out by adding 100 mg of MWS loaded nitrate to 50 mL of NaCl saturated solution. The mixture was stirred for 10 min at room temperature at a stirring rate of 120 rpm. Then, the mixture was passed through Whatman 42 filter paper and the final nitrate concentration in the desorption medium was measured using the spectrophotometer.

Reusability of MWS was tested with five consecutive adsorption-desorption cycles. The reusability experiments were conducted by adding 100 mg of MWS to 50 mL of nitrate solution in a concentration of 20 mg L^{-1}. The mixture was stirred for 10 min at room temperature at a stirring rate of 120 rpm. The MWS loaded nitrate was separated by passing the mixture through the Whatman 42 filter paper. To desorb nitrate, the MWS-loaded nitrate was poured into 50 mL of NaCl saturated solution, and the desorption experiments were carried out under the same conditions as described above. After each desorption experiment, the MWS particles were separated by filtering the mixture. The MWS particles were dried and reused for the next adsorption-desorption cycle. The amount of adsorbed nitrate at each cycle was detected by the spectrophotometer.

RESULTS AND DISCUSSION

Characterization of WS and MWS

The surface morphology of WS and MWS are shown in Figure 1(a) and 1(b). A clear difference is observed between the surface structures of WS and MWS. The FESEM micrograph of WS confirms a rough and irregular surface, while that of MWS demonstrates a uniform and smooth surface. Also, the EDS analyses of WS and MWS show their constitutive elements (see Figure 1(c) and 1(d)). The presence of Si and Cl signals in the MWS EDS spectra verifies the successful functionalization of WS.

Figure 2 shows the TGA analysis curves and FTIR spectra of WS and MWS. As illustrated in Figure 2(a), for WS, a weight loss of around 5% with a slight slope is observed at
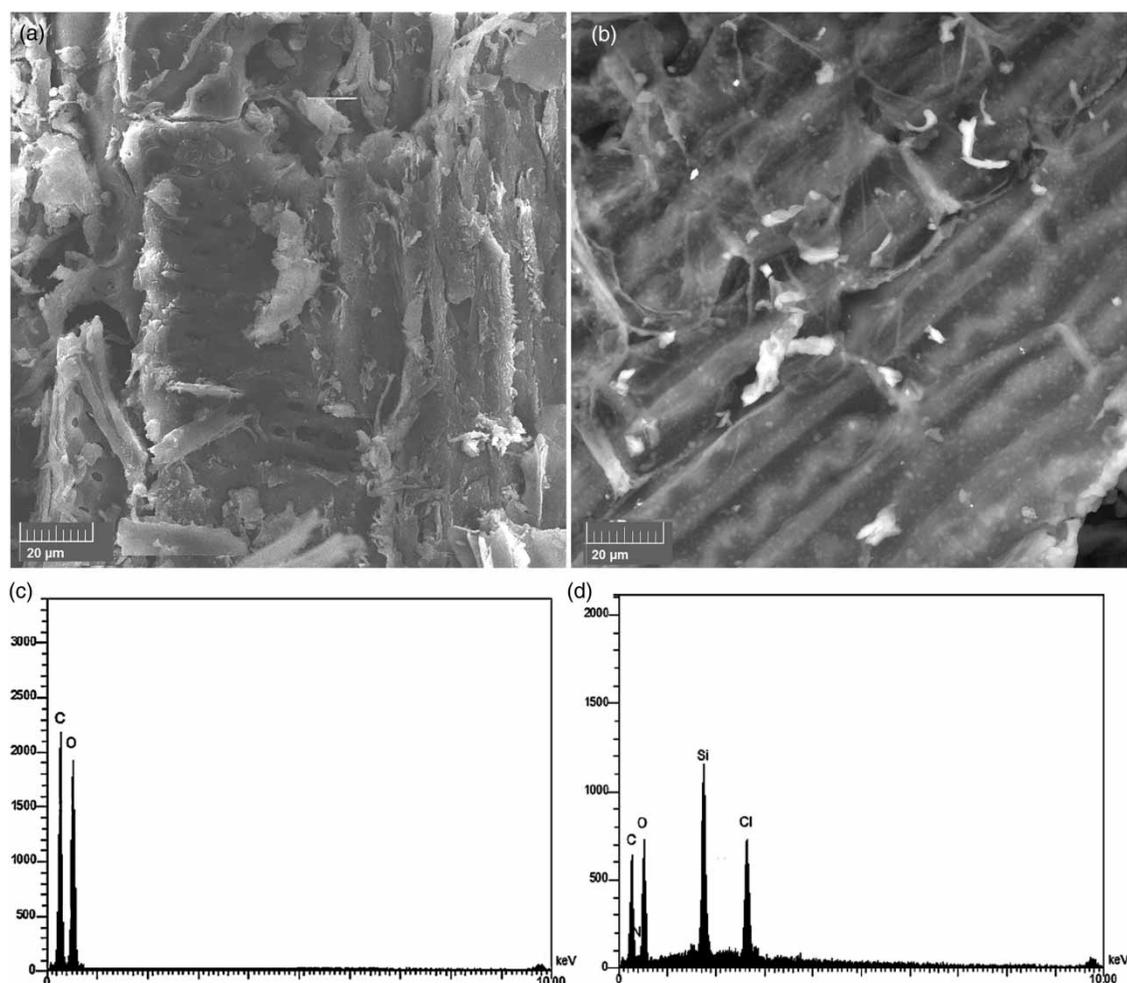
Figure 1 │ FESEM images (above) and EDS curves (below) of WS (a and c) and MWS (b and d).

200 °C, which resulted from moisture evaporation. At temperatures above 200 °C, there is a weight loss of around 70% from 200 °C to 400 °C, which can be due to the thermal degradation of the organic compounds. The char yield is about 10% at 700 °C. For MWS, the around 5% weight loss up to 200 °C is due to moisture evaporation. A weight loss of around 55% occurs from 200 °C to 400 °C, which can be related to the decomposition of the silane groups positioned on the surface of WS. The residual weight of MWS is around 40% at 700 °C. These findings clearly demonstrate that the network structure of MWS leads to higher thermal stability of MWS in comparison with WS.

Figure 2(b) shows that adsorption peak at 1,047 cm^{-1} is assigned to the stretching vibration of C–O bonding in WS, while the adsorption peak at 1,089 cm^{-1} is assigned to the stretching vibration of C–O and Si-O bonding in MWS. The broad adsorption peak of –OH bonding of WS and MWS is extended at ~3,500 cm^{-1}. The adsorption peaks around 2,906 and 2,927 cm^{-1} are assigned to the stretching vibration of C-H bonding of WS and MWS, respectively. The difference between the intensity of the adsorption bands and the alignment of the adsorption peaks demonstrates that the modification process of WS and MWS formation was successful.

Influences of various operational factors on nitrate removal by MWS

Influence of initial solution pH

The influence of the initial solution pH on nitrate removal by MWS was studied at pH values of 3, 5, 7, 9 and 11 under the conditions specified in Table 1. The pH value was adjusted using 0.1 M HCl and 0.1 M NaOH. Figure 3(a) shows that there are slight variations in nitrate removal efficiency at pHs of 3 to 9. However, the removal efficiency
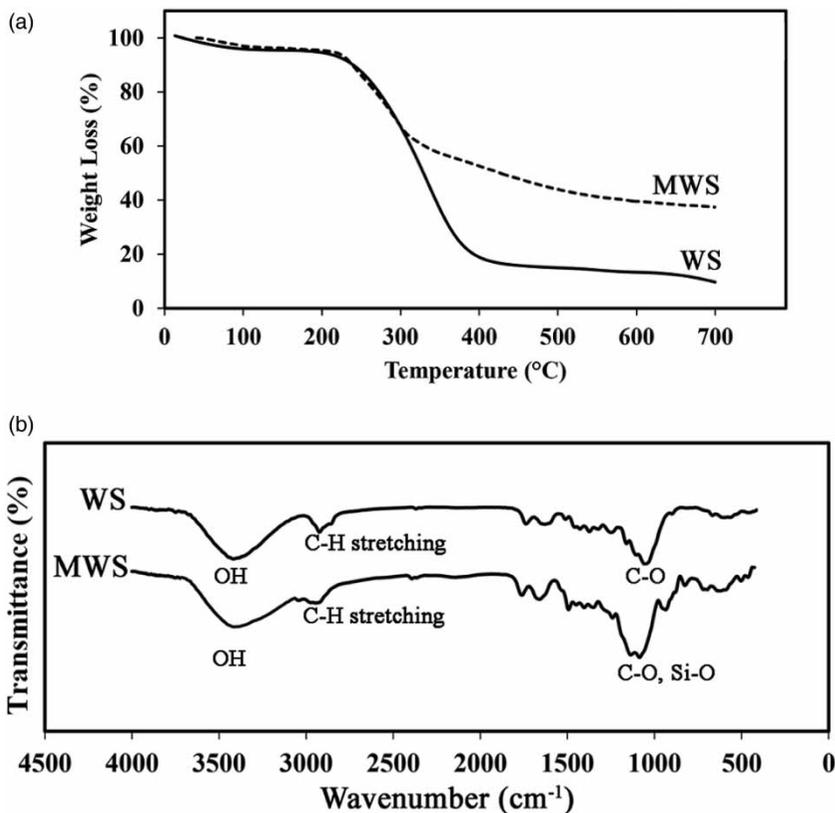
Figure 2 │ TGA curves (a) and FTIR spectra (b) of WS and MWS.

dramatically decreases with the increase of pH from 9 to 11. Thus, the MWS can efficiently remove nitrate from water in a wide range of pHs and the removal efficiency achieves a maximum (81.50%) at pH of 7. The slight decrease in the removal efficiency at the acidic pHs is probably related to the competition between Cl^- and NO_3^- anions for MWS active sites (Milmile *et al.* 2011; Mazarji *et al.* 2017). In fact, the concentration of the Cl^- anion in the nitrate solution increases at the acidic pHs due to the addition of 0.1 M HCl to the solution. In this case, the nitrate removal efficiency decreases because of the inhibitory effect of the Cl^- anion, which will be demonstrated in the study of the effect of the competing anions. The decrease in the removal efficiency at the alkaline pHs might be due to the increase in the negative charged sites, the competition between OH^- and NO_3^- anions for the MWS active sites, and the inter-action during passive transport in the pores (Xu *et al.* 2013; Mazarji *et al.* 2017). Attaining the maximum removal efficiency at the pH of 7 is valuable from the practical point of view because the pH of natural water is usually neutral (pH = 7). Therefore, nitrate removal from natural water by MWS is not required to adjust the pH, which reduces the cost of water treatment and facilitates the application of

this adsorbent. According to the results obtained in this sub-section, the pH of 7 was selected to conduct the other batch experiments throughout this work.

Influence of contact time

The nitrate adsorption rate onto MWS was examined up to a contact time of 50 min under the experimental conditions given in Table 1. It is evident from Figure 3(b) that the nitrate adsorption capacity increases rapidly from 0 mg g^{-1} to 7.6 mg g^{-1} during the first 2 min of the experiment. After this rapid stage, the nitrate adsorption capacity increases rather slowly from 7.6 mg g^{-1} at a time of 2 min to 8.35 mg g^{-1} at a time of 10 min. The high initial adsorp-tion rate might to be due to the high number of available adsorption sites and the high concentration gradient between the nitrate in the solution and the adsorbent surface during the initial adsorption stage. Perceivably, these active sites and concentration gradient decrease gradually over experimental time, which declines the adsorption rate and finally equilibrium is attained. As observed in Figure 3(b), the adsorption capacity reaches approximately a constant value at a time of 10 min and it does not increase with
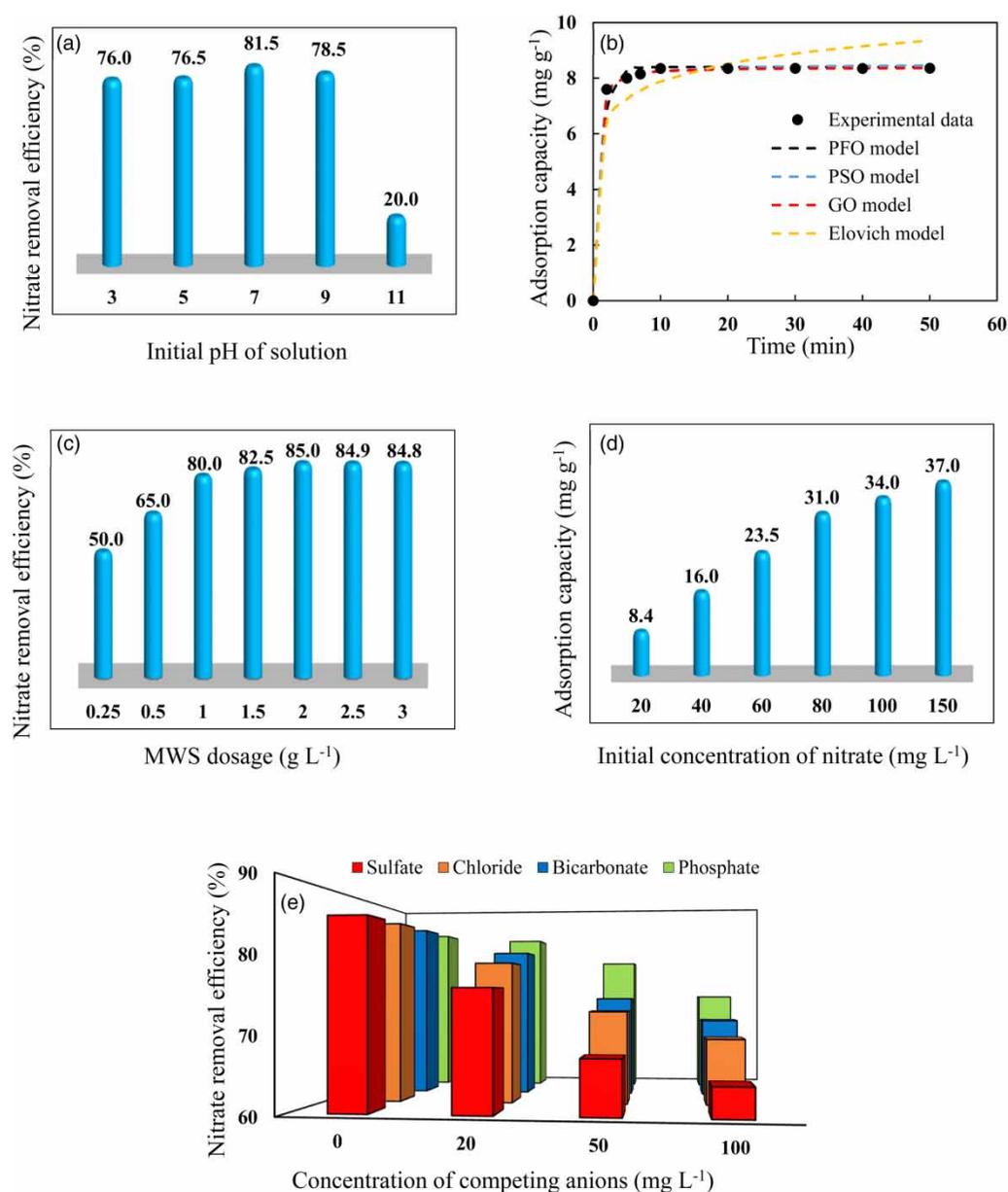
Figure 3 │ Influences of different operational conditions on nitrate removal by MWS. (a) Initial pH of solution, (b) contact time, (c) MWS dosage, (d) initial concentration of nitrate, and (e) competing anions.

increasing contact time after 10 min. Therefore, the time of 10 min was considered as the equilibrium contact time and used in the other batch experiments. Compared to some adsorbents reported in the literature (e.g. Divband Hafshejani *et al.* 2016; Mazarji *et al.* 2017), the MWS requires less contact time to remove nitrate from water.

Influence of adsorbent dosage

The effect of MWS dosage in enhancing the removal percentage of nitrate was investigated using different dosages in

the range of $0.25–3\,\mathrm{g\,L^{-1}}$ and under the operational conditions mentioned in Table 1. As observed in Figure 3(c), the efficiency of the nitrate removal increases significantly from 50% to 82.5% with increasing the MWS dosage from $0.25\,\mathrm{g\,L^{-1}}$ to $1\,\mathrm{g\,L^{-1}}$, while the efficiency increases only from 82.5% to 85% with increasing the MWS dosage from $1\,\mathrm{g\,L^{-1}}$ to $2\,\mathrm{g\,L^{-1}}$. The much enhancement of the nitrate adsorption onto MWS in the range of $0.25\,\mathrm{g\,L^{-1}}$ to $1\,\mathrm{g\,L^{-1}}$ can be resulted from increasing exchangeable area and greater amount of available adsorbent sites (Milmile *et al.* 2011). However, the less improvement of nitrate adsorption

in the range of $1\,g\,L^{-1}$ to $2\,g\,L^{-1}$ can be attributed to the conglomeration of the exchanger particles at high dosages of adsorbent, which leads to decrease effective surface area of adsorbent (Katal *et al.* 2012). As seen in Figure 3(c), the efficiency of the nitrate removal attains to a maximum value (85%) at the MWS dosage of $2\,g\,L^{-1}$. Thereafter, the efficiency remains almost constant and does not increase with the further increase of MWS dosage. Therefore, the MWS dosage of $2\,g\,L^{-1}$ was selected as the optimum dosage and the next batch experiments were carried out at this dosage. The optimum dosage obtained for MWS is less than the other adsorbents applied to remove nitrate from water (e.g. Katal *et al.* 2012; Sepehri *et al.* 2014; Mazarji *et al.* 2017).

Influence of initial nitrate concentration

To examine the effect of the initial nitrate concentration on the adsorption capacity of nitrate by MWS, the batch experiments were conducted by varying the concentration of nitrate solution from $20\,mg\,L^{-1}$ to $150\,mg\,L^{-1}$ at the conditions given in Table 1. According to the obtained results, the adsorption capacity of nitrate increases with increasing the initial nitrate concentration (see Figure 3(d)). A detailed investigation of Figure 3(d) reveals that the adsorption capacity increases from $8.4\,mg\,g^{-1}$ to $31\,mg\,g^{-1}$ when the initial nitrate concentration increases from $20\,mg\,L^{-1}$ to $80\,mg\,L^{-1}$, while it increases only from $31\,mg\,g^{-1}$ to $37\,mg\,g^{-1}$ when the initial nitrate concentration increases from $80\,mg\,L^{-1}$ to $150\,mg\,L^{-1}$. Similar results have been observed in the literature corresponded to the nitrate removal from water using various adsorbents (e.g. Milmile *et al.* 2011; Divband Hafshejani *et al.* 2016; Tong *et al.* 2017). The much increase of adsorption capacity in the range of $20\,mg\,L^{-1}$ to $80\,mg\,L^{-1}$ can be resulted from the increase of nitrate concentration gradient between the bulk liquid phase and the MWS surface (Milmile *et al.* 2011). This phenomenon increases the driving force and improves the adsorption behavior of MWS. On the other hand, the less increase of the adsorption capacity in the range of $80\,mg\,L^{-1}$ to $150\,mg\,L^{-1}$ may be due to the lack of the adsorption active sites and the saturation of them by nitrate ions at high initial concentrations (Divband Hafshejani *et al.* 2016; Tong *et al.* 2017).

Influence of competing anions

Since the nitrate-contaminated water maybe contains other anions that might compete with nitrate for active sites, it is necessary to evaluate the effect of the competing anions. This work was conducted at University of Kurdistan, Sanandaj, in Iran's west. According to the previous studies (e.g. Jalali 2007; Sharifi & Safari Sinegani 2012), the predominant anions in water resources of Iran's west include nitrate (NO_3^-), sulfate (SO_4^{-2}), chloride (Cl^-), bicarbonate (HCO_3^-) and phosphate (PO_4^{-3}). Therefore, in this study, the competition effects of sulfate, chloride, bicarbonate and phosphate were investigated. To this end, the batch experiments were carried out at various concentrations of competing anions (20, 50 and $100\,mg\,L^{-1}$) under the conditions specified in Table 1. The concentrations of competing anions were approximately considered according to previous studies (Divband Hafshejani *et al.* 2016; Tong *et al.* 2017) because the wide ranges have been reported for the concentration changes of above mentioned anions in water resources of Iran's west.

As shown in Figure 3(e), the competing anions reduce the removal efficiency of nitrate in the order of sulfate > chloride > bicarbonate> phosphate. Several previous studies have reported that sulfate have had maximum inhibition effect on the nitrate adsorption, followed by chloride (e.g. Cho *et al.* 2011; Rezaei Kalantary *et al.* 2016; Mazarji *et al.* 2017; Tong *et al.* 2017). The inhibition effect of sulfate can be related to this fact that the bivalent anions had more adsorption tendency than monovalent ones (Rezaei Kalantary *et al.* 2016). However, the inhibition effect of chloride can be resulted from greater tendency of chloride to undergo ion exchange reaction compared to bicarbonate and phosphate (Cho *et al.* 2011). Also, the performance of the batch experiments at pH of 7 may be the responsible for the minimum inhibition effect of phosphate because the monovalent phosphate anion ($H_2PO_4^-$) is the predominant species of phosphate ion at pH of 6 to 7 (Loganathan *et al.* 2013).

Adsorption kinetic modeling and mechanism

Figure 3(b) shows the fitting curves of the kinetic models for nitrate adsorption onto MWS. Also, Table 2 lists the fitting parameters of the models and the associated statistical criteria. As observed in Table 2, the general-order (GO) model has the lowest values of Chi^2/df and F_{error}, and the highest value of R^2_{adj} in comparison with the other kinetic models. In addition, the estimated q_e value in the Go model is relatively closer to the experimental one in comparison with the obtained q_e values in the pseudo-first order (PFO) and pseudo-second order (PSO) models. These confirm that the GO model better describes the

kinetic of nitrate adsorption onto MWS. The better fit of the kinetic data to the GO model implies the order of the adsorption process should follow the same pattern as the chemical reaction (Alencar *et al.* 2012). Table 2 presents the values of h_0 obtained with PFO, PSO and GO models. However, the values of h_0 calculated by the GO model is more confident because the kinetic data are better fitted to this model (Alencar *et al.* 2012).

Figure 4 illustrates the plot of the IPD model (q_t versus $t^{0.5}$) for nitrate adsorption onto MWS. This plot includes three distinct linear sections, which indicate the presence of three consecutive steps in the adsorption process (Alencar *et al.* 2012; Tran *et al.* 2017): The first section, which has the steepest slope and is completed in the first 2 min of the adsorption process, describes film diffusion of nitrate ions from the bulk liquid phase to the adsorbent external surface. The second section, which is completed in up to 10 min, has a lesser slope in comparison with the first one. This section represents IPD where nitrate ions diffuse from the exterior of the adsorbent into pores of the adsorbent. The last section, which starts after 10 min, is related to the final equilibrium stage. In this stage, the IPD begins to slow down and an apparent saturation takes place. Also, since the plot of q_t versus $t^{0.5}$ doesn't pass through the origin, the adsorption process is controlled by both film diffusion and IPD simultaneously (Tran *et al.* 2017).

Adsorption equilibrium modeling

The equilibrium adsorption data of nitrate onto MWs were fitted to the Langmuir, Freundlich and Redlich–Peterson isotherm models. Table 2 gives the fitting parameters of the models and the corresponding statistical criteria. As can be seen in Table 2, the most appropriate values of the statistical criteria belong to the Langmuir isotherm model followed by the Redlich–Peterson isotherm model. Figure 5, which depicts the fitting curves of the isotherm models, confirms this finding. Therefore, the Langmuir isotherm model explains satisfactorily the adsorption process of nitrate onto MWS. This suggests the MWS is structurally homogeneous, in which all adsorption sites are identical and energetically equivalent (Parab & Sudersanan 2010). Therefore, the adsorption process is monolayer and is restricted by the saturation of the adsorption sites (Song *et al.* 2016). It is also necessary to mention that the calculated maximum adsorption capacity by the Langmuir isotherm model in this work ($q_{max} = 47.95$ mg g^{-1}) is more than those reported in the literature (e.g. Sepehri *et al.* 2014; Divband Hafshejani *et al.* 2016; Mazarji *et al.* 2017).

Table 2 │ Kinetic and isotherm parameters of nitrate adsorption onto MWS

Kinetic models

Model					R^2_{adj}	Chi²/df (%)	F_{error} (%)
PFO model	$q_{e, exp}$ (mg g^{-1}) 8.35	$q_{e, cal}$ (mg g^{-1}) 8.40	k_1 (min^{-1}) 0.83	h_0 (mg g^{-1} min^{-1}) 6.97	0.85	1.81	4.65
PSO model	$q_{e, exp}$ (mg g^{-1}) 8.35	$q_{e, cal}$ (mg g^{-1}) 8.51	k_2 (g mg^{-1} min^{-1}) 0.39	h_0 (mg g^{-1} min^{-1}) 28.24	0.98	0.15	1.39
GO model	$q_{e, exp}$ (mg g^{-1}) 8.35	$q_{e, cal}$ (mg g^{-1}) 8.38	K_n ((g mg^{-1})$^{n-1}$ min^{-1}) 0.63; n 1.80	h_0 (mg g^{-1} min^{-1}) 28.92	0.99	0.04	0.78
Elovich model	$q_{e, exp}$ (mg g^{-1}) 8.35	β (g mg^{-1}) 1.09	α (mg g^{-1} min^{-1})		0.11	9.81	10.81

Isotherm models

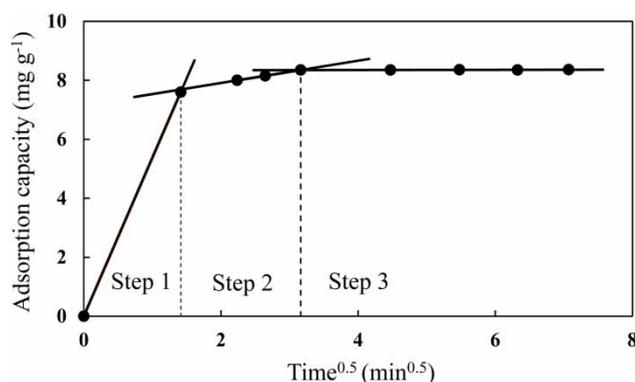| Model				R^2_{adj}	Chi²/df (%)	F_{error} (%)
Langmuir model	q_{max} (mg g^{-1}) 47.95	b (L mg^{-1}) 0.07		0.90	32.33	10.40
Freundlich model	K_F (mg g^{-1} (mg L^{-1})$_F^{-1/n}$) 5.81	n_F 2.11		0.52	167.16	23.39
Redlich–Peterson model	K_{RP} (L g^{-1}) 3.75	a_{RP} ((mg L^{-1})$^{-g}$) 0.12	g 0.90	0.77	65.81	14.63

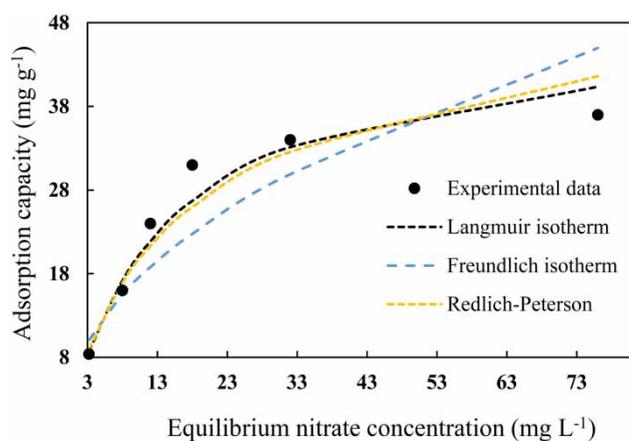**Figure 4** │ IPD model for nitrate adsorption by MWS.

Figure 5 │ Fitting curves of equilibrium isotherms for nitrate adsorption by MWS.

Considering the Langmuir isotherm model describes well the equilibrium adsorption data, a separation factor (R_L) was calculated. For more detail about R_L, the interested reader is referred to Tran et al. (2017) and the references cited therein.

In this study, the values of R_L vary in the range of 0.087 to 0.417. Therefore, the adsorption process of nitrate onto MWS is favorable. As observed in Figure 5, fitted curves to the equilibrium adsorption data by the Langmuir and Redlich–Peterson isotherm models are very close to each other. This results from the fact that the value obtained for the exponent of the Redlich–Peterson isotherm model ($g = 0.90$) is near 1. In this case, this model extremely approaches the Langmuir isotherm model (Wu et al. 2010).

Influence of temperature and thermodynamic parameters

To clarify the effect of temperature on nitrate adsorption by MWS, the batch experiments were performed at room temperature (~25 °C), 35 °C and 50 °C under the conditions mentioned in Table 1. According to the obtained results (see Table 3), both the adsorption capacity and the removal efficiency of nitrate decrease with increasing temperature. This suggests that the low temperature is favorable to remove nitrate by MWS and the adsorption process is exothermic (Katal et al. 2012). The decrease in the nitrate adsorption by MWS with increasing temperature from 35 °C to 50 °C can be related to either increasing the desorption tendency of nitrate ions from the solid-solution interface to the bulk solution, or damaging the active binding sites of MWS. However, the decrease in the nitrate adsorption with increasing temperature from 25 °C to 35 °C can result from increasing the mobility of nitrate ions (Bhatnagar & Sillanpää 2011).

The above-mentioned temperature effects were further examined by calculating the thermodynamic parameters. Table 3 presents the corresponding thermodynamic parameters. As observed, the signs of all thermodynamic parameters are negative. The negative $\Delta H°$ value implies the exothermic nature of the adsorption process, while the negative $\Delta S°$ value demonstrates a decreased randomness at the solid-liquid interface during the nitrate adsorption process. The negative $\Delta G°$ values at different temperatures indicate that the nitrate adsorption onto MWS is a feasible and spontaneous process (Mazarji et al. 2017). The decrease in the magnitude of $\Delta G°$ implies that the low temperature favors nitrate adsorption onto MWS (Tong et al. 2017). This finding is consistent with the decreasing effect of the temperature increase on the nitrate removal by MWS which was mentioned above.

Desorption efficiency and reusability of MWS

According to the results of desorption experiments, on average, 97.3% of the adsorbed nitrate is desorbed from MWS using NaCl saturated solution as a desorption agent. Figure 6

Table 3 │ Effect of temperature and thermodynamic parameters of nitrate adsorption onto MWS

	Temperature (K)		
	298.15	308.15	323.15
q_e (mg g^{-1})	8.40	5.80	2.00
R (%)	84	58	20
$\Delta H°$ (kJ mol^{-1})	−119.85		
$\Delta S°$ (J K^{-1} mol^{-1})	−355.90		
$\Delta G°$ (kJ mol^{-1})	−19.52	−16.75	−12.77

shows the nitrate removal efficiencies by MWS over five successive adsorption-desorption cycles. As evident from Figure 6, the removal efficiencies slightly decreased (by about 2.4%) after five adsorption-desorption cycles. This decrease can be related to the negligible loss of MWS during the adsorption-desorption process. These results reveal that the MWS offers a high potential to be used repeatedly in removing nitrate from water without considerable decrease in its removal efficiency.

CONCLUSIONS

In this study, wheat straw (WS), a plentiful agricultural by-product in Iran, was modified using 3-chloropropyl-trimethoxysilane (CPTMS) and (1,4-diazabicyclo[2.2.2] octane) (DABCO) for the first time and applied to remove nitrate from water. Analyses of FTIR and TGA demonstrated the successful modification of WS and the thermal stability of the MWS, respectively. In addition, the analyses of FESEM and DES indicated the morphological and structural differences of WS and MWS. The results of the batch experiments indicated that the optimum conditions of the nitrate adsorption by MWS included: initial nitrate concentration $= 20$ mg L^{-1}, initial solution pH $= 7$, contact time $= 10$ min, MWS dosage $= 2$ g L^{-1} and temperature ≈ 25 °C. Under the optimum conditions, the MWS removed 85% of nitrate from water. The general-order (GO) model showed good agreement with the kinetic adsorption data and the adsorption process consisted of three distinct stages. The Langmuir isotherm fitted well to the equilibrium adsorption data and the values of separation factors (from 0.087 to 0.417) implied the favorability of the adsorption process. The inhibition effect of competing anions was the greatest for sulfate, followed by chloride, bicarbonate and phosphate. Based on the thermodynamic studies, the adsorption
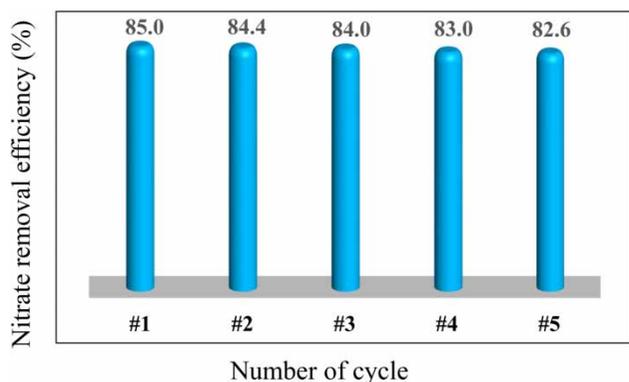
process is exothermic, feasible and spontaneous in nature. In summary, the results of this study demonstrated that the MWS required the simplest operating conditions for nitrate removal. Therefore, it is proposed to investigate the ability of MWS to remove nitrate from natural water resources.

ACKNOWLEDGEMENTS

REFERENCES

Alencar, W. S., Acayanka, E., Lima, E. C., Royer, B., de Souza, F. E., Lameira, J. & Alves, C. N. 2012 Application of *Mangifera indica* (mango) seeds as a biosorbent for removal of Victazol Orange 3R dye from aqueous solution and study of the biosorption mechanism. *Chemical Engineering Journal* **209**, 577–588.

Bergquist, A. M., Choe, J. K., Strathmann, T. J. & Werth, C. J. 2016 Evaluation of a hybrid ion exchange-catalyst treatment technology for nitrate removal from drinking water. *Water Research* **96**, 177–187.

Bhatnagar, A. & Sillanpää, M. 2011 A review of emerging adsorbents for nitrate removal from water. *Chemical Engineering Journal* **168**, 493–504.

Cho, D.-W., Chon, C.-M., Kim, Y., Jeon, B.-H., Schwartz, F. W., Lee, E.-S. & Song, H. 2011 Adsorption of nitrate and Cr(VI) by cationic polymer-modified granular activated carbon. *Chemical Engineering Journal* **175**, 298–305.

Divband Hafshejani, L., Hooshmand, A., Naseri, A. A., Soltani Mohammadi, A., Abbasi, F. & Bhatnagar, A. 2016 Removal of nitrate from aqueous solution by modified sugarcane bagasse biochar. *Ecological Engineering* **95**, 101–111.

Ebrahimian Pirbazari, A., Saberikhah, E. & Habibzadeh Kozani, S. S. 2014 Fe$_3$O$_4$–wheat straw: preparation, characterization and its application for methylene blue adsorption. *Water Resources and Industry* **7–8**, 23–37.

FAOSTAT 2013 *Food and Agriculture Organization of the United Nations*. Statistics Division, http://faostat3.fao.org/compare/E.

Jalali, M. 2007 Hydrochemical identification of groundwater resources and their changes under the impacts of human activity in the Chah basin in Western Iran. *Environmental Monitoring and Assessment* **130**, 347–364.

Katal, R., Sharifzadeh Baei, M., Taher Rahmati, H. & Esfandian, H. A. 2012 Kinetic, isotherm and thermodynamic study of nitrate adsorption from aqueous solution using modified rice husk. *Journal of Industrial and Engineering Chemistry* **18**, 295–302.

Keränen, A. 2017 *Water Treatment by Quaternized Lignocellulose*. PhD thesis, University of Oulu, Oulu, Finland.

Li, J.-H., Lv, G.-H., Bai, W.-B., Liu, Q., Zhang, Y.-C. & Song, J.-Q. 2016 Modification and use of biochar from wheat straw

Figure 6 | Reusability of MWS with repeated adsorption-desorption cycles.

(Triticum aestivum L.) for nitrate and phosphate removal from water. *Desalination and Water Treatment* **57**, 4681–4693.

Lima, É. C., Adebayo, M. A. & Machado, F. M. 2015 Kinetic and Equilibrium Models of Adsorption. In: *Carbon Nanomaterials as Adsorbents for Environmental and Biological Applications* (C. P. Bergmann & F. M. Machado, eds). Springer, Heidelberg, Germany, pp. 33–69.

Loganathan, P., Vigneswaran, S. & Kandasamy, J. 2013 Enhanced removal of nitrate from water using surface modification of adsorbents – a review. *Journal of Environmental Management* **131**, 363–374.

Mazarji, M., Aminzadeh, B., Baghdadi, M. & Bhatnagar, A. 2017 Removal of nitrate from aqueous solution using modified granular activated carbon. *Journal of Molecular Liquids* **233**, 139–148.

Milmile, S. N., Pande, J. V., Karmakar, S., Bansiwal, A., Chakrabarti, T. & Biniwale, R. B. 2011 Equilibrium isotherm and kinetic modeling of the adsorption of nitrates by anion exchange Indion NSSR resin. *Desalination* **276**, 38–44.

Najafi, G., Ghobadian, B., Tavakoli, T. & Yusaf, T. 2012 Potential of bioethanol production from agricultural wastes in Iran. *Renewable and Sustainable Energy Reviews* **13**, 1418–1427.

Parab, H. & Sudersanan, M. 2010 Engineering a lignocellulosic biosorbent – coir pith for removal of cesium from aqueous solutions: equilibrium and kinetic studies. *Water Research* **44**, 854–860.

Rezaei Kalantary, R., Dehghanifard, E., Mohseni-Bandpi, A., Rezaei, L., Esrafili, A., Kakavandi, B. & Azari, A. 2016 Nitrate adsorption by synthetic activated carbon magnetic nanoparticles: kinetics, isotherms and thermodynamic studies. *Desalination and Water Treatment* **57**, 16445–16455.

Sepehri, S., Heidarpour, M. & Abedi-Koupai, J. 2014 Nitrate removal from aqueous solution using natural zeolite-supported zero-valent iron nanoparticles. *Soil and Water Research* **9**, 224–232.

Sharifi, Z. & Safari Sinegani, A. A. 2012 Arsenic and other irrigation water quality indicators of groundwater in an agricultural area of Qorveh plain, Kurdistan, Iran. *American-Eurasian Journal of Agriculture & Environmental Sciences* **12**, 548–555.

Song, W., Gao, B., Xu, X., Wang, F., Xue, N., Sun, S., Song, W. & Jia, R. 2016 Adsorption of nitrate from aqueous solution by magnetic amine-crosslinked biopolymer based corn stalk and its chemical regeneration property. *Journal of Hazardous Materials* **304**, 280–290.

Tong, X., Yang, Z., Xu, P., Li, Y. & Niu, X. 2017 Nitrate adsorption from aqueous solutions by calcined ternary Mg-Al-Fe hydrotalcite. *Water Science and Technology* **75**, 2194–2203.

Tran, H. N., You, S.-J., Hosseini-Bandegharaei, A. & Chao, H.-P. 2017 Mistakes and inconsistencies regarding adsorption of contaminants from aqueous solutions: a critical review. *Water Research* **120**, 88–116.

Wang, L. 2012 Application of activated carbon derived from 'waste' bamboo culms for the adsorption of azo disperse dye: kinetic, equilibrium and thermodynamic studies. *Journal of Environmental Management* **102**, 79–87.

Wang, Y., Gao, B.-Y., Yue, W.-W. & Yue, Q.-Y. 2007 Preparation and utilization of wheat straw anionic sorbent for the removal of nitrate from aqueous solution. *Journal of Environmental Sciences* **19**, 1305–1310.

Wang, X., Lü, S., Gao, C., Feng, C., Xu, X., Bai, X., Gao, N., Yang, J., Liu, M. & Wu, L. 2016 Recovery of ammonium and phosphate from wastewater by wheat straw-based amphoteric adsorbent and reusing as a multifunctional slow-release compound fertilizer. *ACS Sustainable Chemistry and Engineering* **4**, 2068–2079.

WHO 2011 *Guidelines for Drinking-Water Quality*, 4th edn. World Health Organization, Geneva, Switzerland.

Wu, F.-C., Liu, B.-L., Wu, K.-T. & Tseng, R.-L. 2010 A new linear form analysis of Redlich–Peterson isotherm equation for the adsorptions of dyes. *Chemical Engineering Journal* **162**, 21–27.

Xu, X., Gao, B.-Y., Tan, X., Yue, Q.-Y., Zhong, Q.-Q. & Li, Q. 2011 Characteristics of amine-crosslinked wheat straw and its adsorption mechanisms for phosphate and chromium (VI) removal from aqueous solution. *Carbohydrate Polymers* **84**, 1054–1060.

Xu, X., Gao, B., Yue, Q., Li, Q. & Wang, Y. 2013 Nitrate adsorption by multiple biomaterial based resins: application of pilot-scale and lab-scale products. *Chemical Engineering Journal* **234**, 397–405.

Xue, L., Gao, B., Wan, Y., Fang, J., Wang, S., Li, Y. & Muñoz-Carpena Yang, L. 2016 High efficiency and selectivity of MgFe-LDH modified wheat-straw biochar in the removal of nitrate from aqueous solutions. *Journal of the Taiwan Institute of Chemical Engineers* **63**, 312–317.